water

MDPI

Article

Study of Flooding Behavior and Discharge from Karot Dam in the Event of a Possible Breach by Using the Hydrodynamic Model

Lilian Thomas Momburi [1,2], Changwen Li [1,2,3,*], Frank N. M. Masami [4], Minglei Ren [3] and Isaac Otoo [1,2]

[1] Hubei Key Laboratory of Construction and Management in Hydropower Engineering, China Three Gorges University, Yichang 443005, China; lylmombury90@gmail.com (L.T.M.); spatboy@yahoo.com (I.O.)
[2] College of Hydraulic and Environmental Engineering, China Three Gorges University, Yichang 443005, China
[3] Key Laboratory of Sediment Science and Northern River Training, the Ministry of Water Resources, China Institute of Water Resources and Hydropower Research, Beijing 100048, China; renml@iwhr.com
[4] Simiyu Climate Resilience Project, GITEC-IGIP GmbH in Association with ICE Project Services Limited, Simiyu 1053, Tanzania; frank.natalis@gmail.com
* Correspondence: lichangwen@alumni.hust.edu.cn; Tel.: +86-135172-54948

Abstract: This study utilizes the MIKE 11 hydrodynamic model developed by the Danish Hydraulic Institute to simulate flood behavior downstream of Karot Dam under multi-year in-flow conditions. The key parameters analyzed include breach characteristics, flood duration, water depth, flow velocity, discharge rate, and downstream distance. After dam failure, the peak discharge reaches 33,171 m^3/s, exceeding the 10,000-year recurrence peak flow of 32,300 m^3/s, with a breach duration of 2 h. The estimated peak discharge after simulation using empirical equations and comparative analyses showed maximum flood discharges of 28,187 m^3/s, 28,922 m^3/s, and 29,769 m^3/s, with breach widths of 181 m, 256 m, and 331 m, respectively. The peak discharge predicted to reach the outlet with travel time ranging from 4 h 25 min to 4 h 40 min. Under multi-year average inflow conditions, Mangla Dam faces no risk of failure, with a maximum outflow of 12,097 m^3/s and a spillway capacity of 30,147 m^3/s. The model accurately predicted discharge values, with a strong correlation coefficient of $R^2 = 0.9653$, indicating strong agreement between the actual water level data and predicted discharge. These insights are essential for developing effective emergency response strategies to mitigate the risks associated with dam failure.

Keywords: asphaltic concrete core; rockfill dam; dam break; hydrodynamic model; multi-year average inflow; peak discharge

Citation: Momburi, L.T.; Li, C.; Masami, F.N.M.; Ren, M.; Otoo, I. Study of Flooding Behavior and Discharge from Karot Dam in the Event of a Possible Breach by Using the Hydrodynamic Model. *Water* **2024**, *16*, 2922. https://doi.org/10.3390/w16202922

Academic Editors: Majid Mohammadian, Xiaohui Yan and Hossein Kheirkhah Gildeh

Received: 26 August 2024
Revised: 8 October 2024
Accepted: 10 October 2024
Published: 14 October 2024

1. Introduction

Dam failure is the collapse or displacement of a portion of a dam or its foundation, rendering the dam incapable of retaining water. Generally, dam failure leads to the release of large volumes of water, posing risks to the properties of downstream residents [1]. Overtopping and piping are common causes of dam failures, and because of their complexity and dearth of information, they can cause a pulse downstream even in the absence of a dam failure [2]. In the last 20 years, catastrophic flooding has occurred due to dam failures. The accurate estimations of inundation levels and the precise timing of the arrival of floodwater at a specific location are also necessary for the development of efficient emergency response strategies [3]. Between the years 2000 and 2009, more than 200 notable dam failures occurred worldwide [4]. The Atatürk Dam in southeast Turkey appears to be in critical condition following two devastating earthquakes that occurred recently, with Richter scale readings of 7.5 and 7.8. Experts predict that if the dam failed, the area adjacent to it may be devastated over approximately 30 square kilometers [5]. Another disaster occurred on 13 September 2023. The CAP briefing notes regarding recent events in Derna, Libya, stated that a heavy downpour caused two dams to collapse, submerging

the entire city and resulting in the deaths of over 2000 people [6]. It was reported that the aftermath of the dam collapse affected communication, electrical cables, and agricultural lands in the impacted area. It is likely necessary to rebuild the dam to prevent future flooding in the city. On 23 July 2018, the Saddle Dam D of the Xe Pian-Xe Namnoy reservoir burst, releasing a torrent of water into villages, forests, and agricultural areas along the Vang Ngao River in Laos and Cambodia. This caused significant material damage and resulted in fatalities [7]. For this reason, all dams need to undergo a dam failure analysis. The cost of evaluating dam failure is insignificant compared to the overall expenses incurred by disasters [8].

Dam failures are commonly initiated by both external and internal erosion mechanisms. Factors such as inadequate spillway capacity, internal erosion, seepage, slope failures, and earthquakes often play a role. In many instances, the failure process starts with a breach, which results in the dam collapsing and the water being released. This analysis concludes by comparing the findings from centrifuge tests with the results of dynamic analysis for the Meijaran Dam [9]. The construction and operation of the 174 m high Quxue asphaltic rockfill dam were examined. Based on structure performance monitoring, an asphaltic concrete core rockfill dam is safe in small valleys with slope supports. The interior erosion did not pose a threat; however, the flexible core is not suitable for high ACEDs in narrow valleys with steep abutments [10].

A recent study analyzed the seismic reaction of a rockfill dam with an asphalt concrete core (ACRD) in Bulgaria using two basic approaches and a comprehensive Finite Element Method (FEM) analysis [11]. Comparisons between the outcomes of different techniques were used to determine whether simpler methods were appropriate for most ACRDs [12]. Environmental friendliness, inherent safety, and labor savings are the three main points of discussion when discussing the future of concrete dams.

Over 200 m high earth and rockfill dams have been constructed worldwide, including the Nurek Dam (300 m), the Lianghekou Dam (295 m), and the Nuozhadu Dam (261.5 m). A substantial hydrostatic pressure differential between the upstream and downstream sections is required to store water and generate electricity, which presents a significant challenge to the impermeability performance of these dams [13]. Abnormal seepage is responsible for about one-third of earth and rockfill dam collapses; therefore, accurately predicting seepage behavior is crucial to ensure safe dam operation [14] in rockfill dams. Seepage piping or overtopping are usually the causes of failure; however, dam crest overflow is more frequently observed [15,16]. The shape of a dam breach can generally be described as rectangular or trapezoidal, and its final magnitude is determined by the material properties of the dam, as well as the topography of the dam site and its cross-section [17].

Sealing is a fundamental component of rockfill dams, where it typically forms the central core, as outlined by [18]. The core's primary role is to prevent water from penetrating the structure, as emphasized by [19]. To minimize seepage, materials with low permeability, such as concrete, asphalt concrete, bitumen, and dense clay, are commonly utilized for the core [20]. The materials used in asphaltic construction are water-insoluble, environmentally friendly, and have not been shown to pose a threat to sources of drinking water [21,22]. In addition, many dams that include an asphaltic concrete core have been constructed in China, Canada, Brazil, Spain, and Iran, which have lately expressed interest in building dams using this material, according to [23,24]. Compared to clay core structures, asphalt concrete core designs maintain more stability under the same loading and material circumstances. Additionally, because the dam can be built faster and it is not impacted by weather, the asphalt concrete core dam design option is more cost-effective than the clay core.

The Karot Dam, which collects water from the Jhelum River, is a primary concern for potential dam failure that could result in loss of life, property, and significant economic impacts. The dam features an impermeable earth core with a transition zone between its interior and exterior sections, while its exterior is covered with a rock shell on both the upstream and downstream sides. Given the extensive damage that floods from dam breaches can cause downstream, it is crucial to monitor the integrity of rockfill dams closely. According to the literature reviewed on dam breaking, numerous researchers have

studied the topic internationally, but none have shown any interest in the Karot Dam. This study was initiated to evaluate the breaching risks because the dam is vital to Pakistan's livelihood. Multi-year average inflow conditions refer to the average water volume entering a reservoir, dam, or river over several years, aiding in the planning and design of structures such as reservoirs and dams. They enable engineers to monitor reservoir levels, assess flow patterns, and predict system performance.

Hydrodynamic modeling is critical for assessing flood risks, particularly in places with limited water resources [25]. It demonstrated its usefulness in the Bharathapuzha River basin, indicating that accurate modelling of dam breaches can significantly improve flood risk management by anticipating flood behavior and repercussions. This study emphasizes the need of advanced modelling techniques in improving flood preparedness and response measures.

Analyzing [26], the dam breaching process using reported failure case data is essential for understanding breaching mechanisms and predicting breach flow hydrographs during emergencies [27]. To improve emergency response, increase public awareness, and direct government planning to mitigate the effects of potential dam breaches and flooding incidents in the area, the accuracy of dam breach flood prediction is essential.

In addition to internal causes such as degradation, dam breaches can result from a variety of external causes, such as landslides and earthquakes [28]. A total of 13 primary causes of dam failure have been identified by the US Army Corps of Engineers' Hydrologic Engineering Center (HEC), including extreme storms, equipment malfunctions, structural damage, and sabotage [29]. Water may spread downstream due to a breach, which is an opening in the dam's structure. Examples of causes of dam failure that have been shown by case studies include seepage, internal erosion (piping), overtopping caused by inadequate freeboard, settlement issues with the upstream slope, and liquefaction caused by earthquakes [30].

This study provides valuable insights into the flooding behavior and discharge scenarios following a potential breach of the Karot Dam. By applying an advanced hydrodynamic model (MIKE 11) to analyze dam failure and breach parameters under multi-year average inflow conditions, this research makes a significant contribution to flood risk assessment and mitigation strategies downstream of the dam.

2. Materials and Methods

2.1. Research Area

Karot Dam is an asphalt concrete core rockfill dam constructed on the Jhelum River in Azad Pattan, Pakistan. The engineering, procurement, and construction contract for the asphaltic concrete core rockfill dam was granted to Yangtze Three Gorges Technology and Economy Development Company, and China Machinery Engineering Cooperation. The dam has an average annual discharge capacity of 819 m^3/s at the full reservoir level of 461 m, with the maximum dam height of 95.5 m. It is primarily used for hydropower generation, water supply, and irrigation. Several housing developments exist downstream of the dam site. The details of Karot Dam and its reservoir are shown below, in Table 1 and Figure 1.

Table 1. General details of Karot Dam.

Dam Type	Asphalt Concrete Core Rockfill Dam
Catchment area	26.7 thousand km^2
Maximum dam height	95.5 m
Total capacity of the reservoir	164.5 million m^3
Average annual discharge	819 m^3/s
Normal water level	461 m
Highest water level	469.5 m
Lowest water level	374 m
Dam crest length	460 m

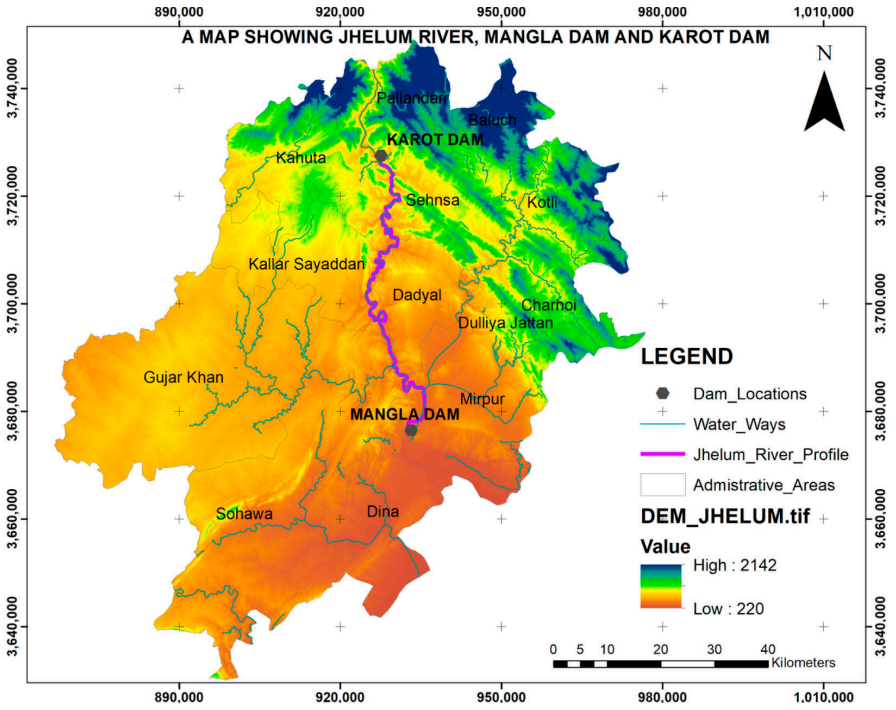

Figure 1. Location of the Jhelum River, showing Karot Dam and Mangla Dam.

2.2. The Numerical Model MIKE 11

MIKE 11's core function is simulating unsteady flow discharge and water levels in rivers and channels. It uses a one-dimensional, implicit finite difference scheme for the numerical solution of the Saint-Venant equations [31].

The flow continuity equation is as follows:

$$\frac{\partial Q}{\partial x} + \frac{\partial A}{\partial t} = q \tag{1}$$

The flow kinematical equation is as follows:

$$\frac{\partial Q}{\partial t} + \frac{\partial (Qv)}{\partial x} + gA\left(\frac{\partial z}{\partial x} + S_f\right) = 0 \tag{2}$$

where:

Q = flow discharge (m^3/s);
v = flow velocity (m/s);
t = time (s);
x = longitudinal distance along the channel (m);
g = gravitational acceleration (9.81 m/s^2);
A = cross-sectional area of flow (m^2);
Z = water surface elevation (m);
S_f = friction slope (energy slope due to friction);
q = lateral inflow (m^2/s).

As the dam-break flood is a water flow movement with very strong non-constancy, the selected numerical format should have the ability to simulate this kind of water flow motion.

In MIKE 11, dispersion is achieved by using a 6-point Abbott central difference format, and the dispersed linear equation set is solved by using the Double Sweep Algorithm shown in Figure 2. On the basis of an implicit, finite difference, the MIKE 11 equations are discretized. These schemes are essential for accurately predicting hydrodynamic behaviors during dam breaches [32].

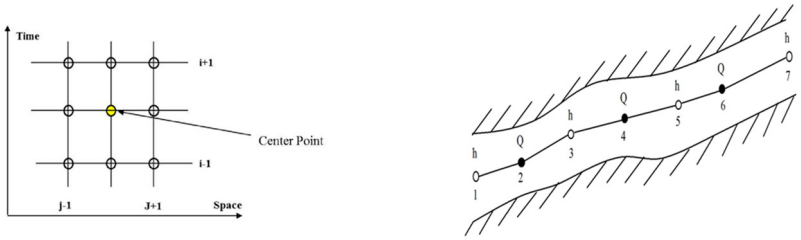

Figure 2. Centered 6-point Abbott scheme and channel section used in the Mike 11 hydrodynamic model for computational purposes.

2.3. Model Setup

The river network module contains certain details about the river channel, including flow direction, computation range, and river mileage, as well as the distance from the Karot Dam site to the Mangla reservoir.

Figure 3 Shows the MIKE 11 model setup for the river network channel, including the location of cross-sections. The developed model has 49 cross-sections with an average section gap of 1.5 km, a 14 km maximum gap of 5.8 km, and a minimum gap of 0.4 km. It spans 72.7 km from the dam site. The 37.5 km long tributaries, made up of 26 sections, have an average section gap of 1.7 km, a maximum gap of 5.3 km, and a minimum gap of 0.3 km within the modeling range (the modelling range was provided by the Hydrology Bureau of Changjiang Water Resources Commission).

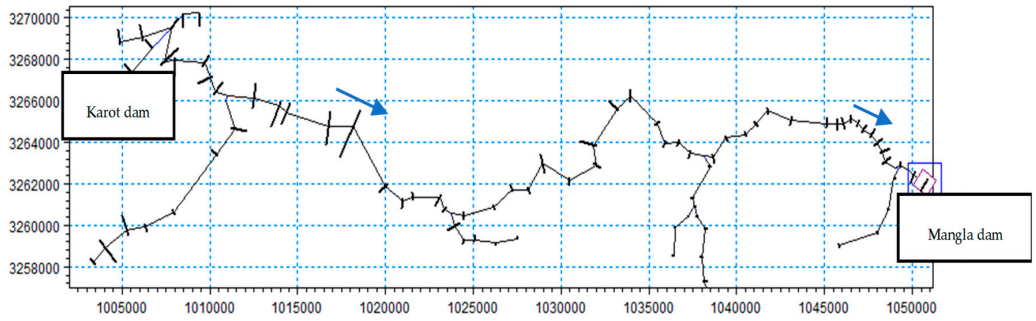

Figure 3. River network channel with location of cross-sections.

Table 2 below shows the design flood outcomes for the Karot Hydropower Station, which were calculated using the P-III distribution and refined through curve-fitting based on an initial estimate from the moment method. It includes key flood data, such as peak values and flood volumes over different durations.

Table 2. The design flood hydrograph at Karot Dam is calculated by amplifying the flood peak, 3 d flood volume, and 7 d flood volume using the same frequency [33]. (SL44-2006 for flood calculations).

	Time Interval	Flood Peak (m^3/s)	3 d Flood Volume (100 Million m^3)	7 d Flood Volume (100 Million m^3)
Frequency curve parameter	Mean value	3550	6.62	3.9
	Cv	0.77	0.6	0.42
	Cs/Cv	4	4	4
Frequency	0.01%	32,300	42.7	57.7
	0.02%	29,600	39.5	54.1
	0.05%	26,000	35.3	49.5
	0.1%	23,400	32.1	45.9
	0.2%	20,700	29	42.3
	0.5%	17,300	24.8	37.6
	1%	14,700	21.7	33.9
	2%	12,200	18.6	30.3
	5%	9020	14.6	25.4
	10%	6740	11.6	21.6
	20%	4660	8.75	17.8

Figure 4 shows a schematic diagram of the dam breach processes of Karot Dam, which occurs when the average annual inflow is sustained over several years, in accordance with related codes and regulations for dam-break flow [34]. The process of a dam breach can be roughly characterized as a trapezoid-shaped gate. As soon as the water level in the Karot hydroelectric station's reservoir reaches the Normal Pool Level of 461 m, the bottom elevation of the dam breach will gradually decrease from 461 m to 410 m over time. Under conditions of multi-year average inflow, the breach width will increase linearly from 0 m to 180 m, with the left- and right-side slopes maintained at a ratio of 1:1.5 (vertical/horizontal). This trapezoidal dam breach shape will persist for two hours.

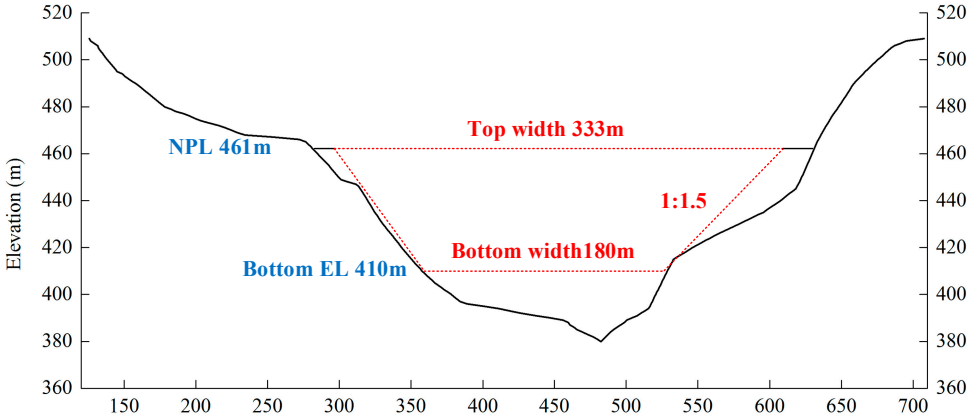

Figure 4. Schematic diagram of the Karot Dam breach process, under the condition of multi-year average inflow.

3. Results and Discussion

The Karot Hydropower Station is a Class II large hydroelectric project featuring a core rockfill dam, with asphalt concrete serving as the water retention structure. According to the Karot Dam-break modeling results in the "Feasibility Study of the 720 MW Karot Hydropower Project," the entire breach formation time is estimated at 2 h. This report analyzes breach durations ranging from 1 to 24 h under multi-year average discharge conditions, from 1 April 1969 to 2010, excluding data from 1993 [33]. ("Regulation for calculating design flood of water resources and hydropower projects" (SL44-2006)). This study examines the sensitivity of several factors, including peak discharge, the highest downstream flood water surface profile, the one-way maximum velocity flow process from the dam site to downstream, and flood peak timing, corresponding to the dam breach duration under multi-year average inflow conditions.

3.1. Peak Discharge Analysis

At the Karot Dam site, Figure 5 illustrates the discharge process under different dam-break durations, while Figure 6 shows the same processes under varying durations. It is evident that, immediately after the dam break, the Karot Dam site experiences a high peak discharge initially, but the flood peak duration is short. Peak discharge decreases by 70,670 m^3/s, from 89,671 m^3/s to 19,001 m^3/s, as the dam-break duration increases from 1 to 24 h. Peak discharge declines rapidly with shorter breach times when the break lasts less than two hours, but increases in peak discharge become negligible if the duration exceeds 10 h.

Figure 7, shows that the peak discharge of the dam-break flood attenuates quickly along its path, decreasing by 12,801 m^3/s, from 33,171 m^3/s to 20,370 m^3/s. After this attenuation, the flood discharge closely resembles that of a natural flood with a 500-year recurrence interval (20,700 m^3/s). Beyond the 40 km range downstream of Karot Dam lies the Mangla reservoir area and a river network with intersecting tributaries.

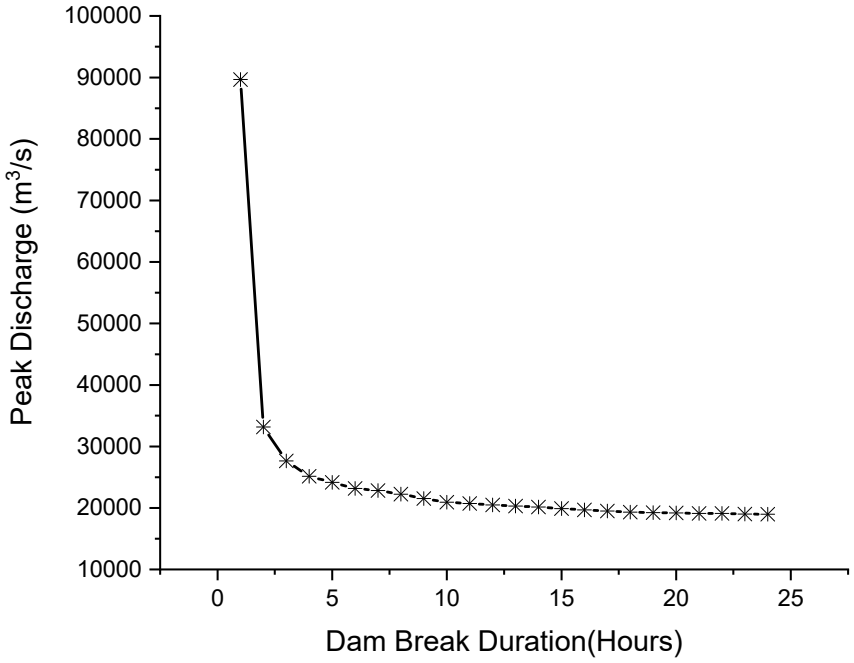

Figure 5. Peak discharge processes under different dam-break durations.

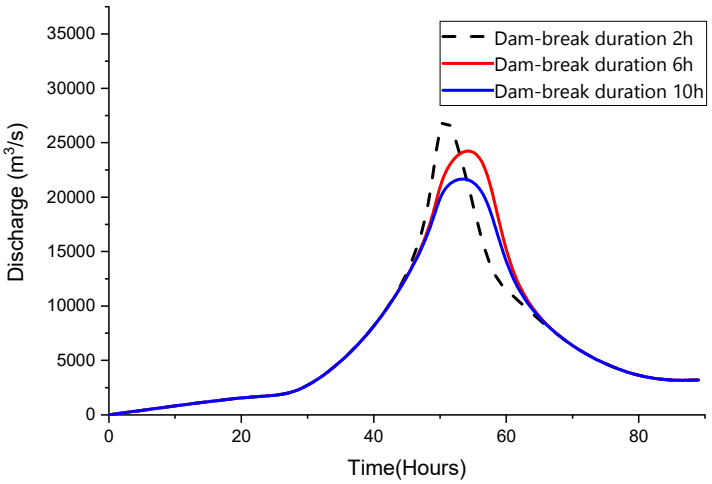

Figure 6. Peak discharge processes under varying dam-break duration.

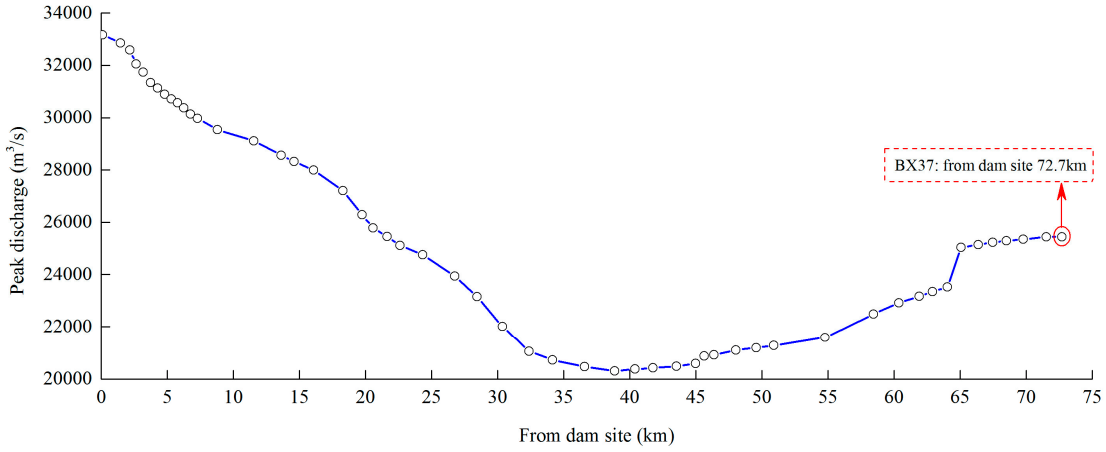

Figure 7. Peak discharge along the downstream section after the dam break.

3.2. Maximum Flood Water Surface Profile Downstream of the Dam and Water Level Process at Various Downstream Typical Sections

Figure 8 shows that as the dam-break duration increases from 1 to 10 h, the highest water levels between Karot Dam and Mangla Dam decrease, particularly from 45 km downstream. The peak discharge at the 45 km mark is reduced due to the influence of the river network, Mangla reservoir, and tributaries, which disperse the flood water and lower the peak.

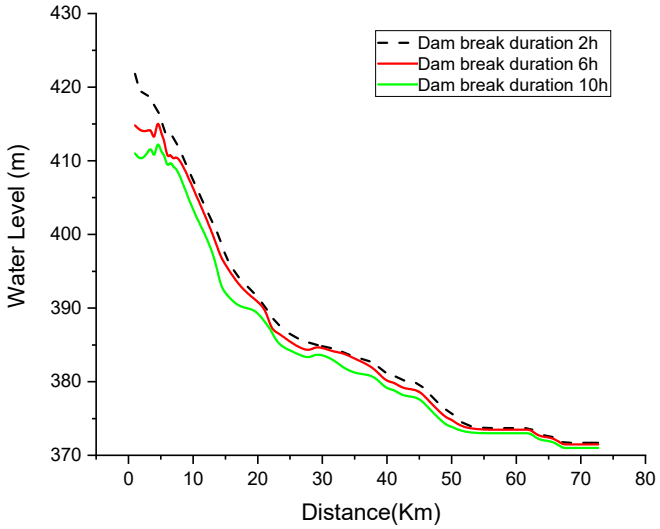

Figure 8. Water level process of different typical sections at downstream of the dam.

Figure 9 shows that the peak discharge of 12,097 m^3/s from the flood caused by the dam collapse at the Mangla dam site is significantly lower than the maximum discharge capacity of 30,147 m^3/s for the normal spillway of the Mangla Hydropower Station under Normal Pool Level (NPL). According to the dispatching schemes of the Mangla Hydropower Station, the reservoir water level can be maintained at the Normal Pool Level (378.56 m).

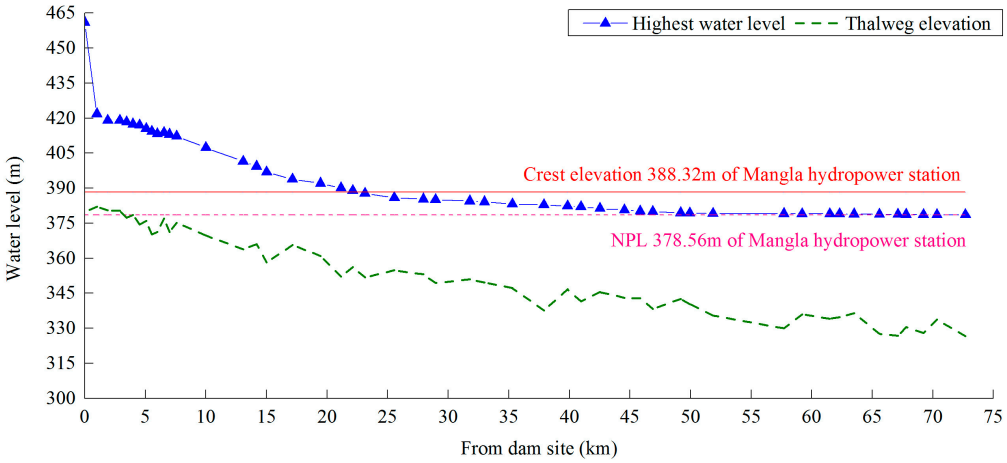

Figure 9. Downstream maximum flood water surface profile after the Karot Dam break.

3.3. The One-Way Maximum Velocity Flow Process from the Dam Site to Downstream

Under the condition of multi-year average inflow, the velocity flow process downstream after the Karot Dam failure is shown in Figure 10. The one-way maximum velocity downstream of the dam decreases significantly. After the dam break, the one-way maximum velocity decreases from 11.8 m/s to 3.4 m/s (0–26 km). Further downstream, between 52 km and 73 km, the maximum velocity sharply declines from 1.2 m/s to 0.1 m/s due to the increased river section area, the Mangla reservoir storage, and the tributaries, which affect the flow magnitude.

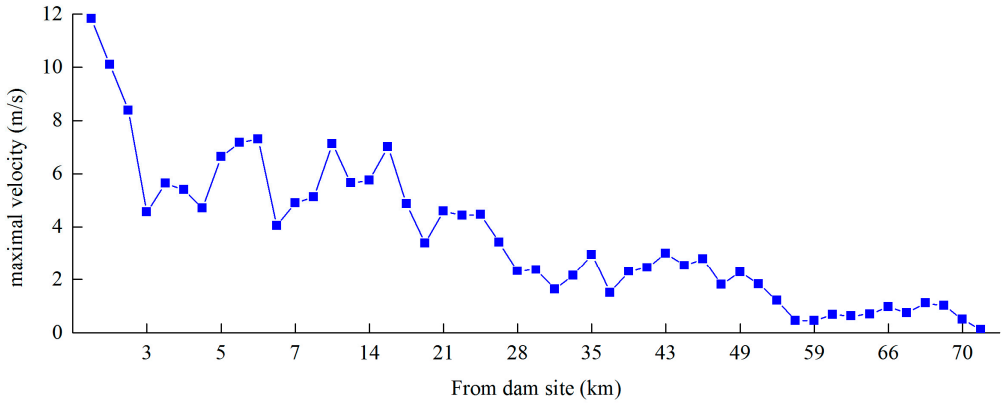

Figure 10. One-way maximum velocity at downstream of Karot Dam.

3.4. Flood Peak Appearance Time

Figure 11 shows the dam break-out flow at different river cross-sections' flood attenuation hydrographs and the one-way discharge process of a typical downstream section of the dam following the Karot Dam break under multi-year average inflow conditions. The dam-break flood propagates rapidly, as reflected by the time it takes for the flood peak to appear. The flood peak reaches locations 12 km, 20 km, 50 km, and 73 km downstream of the dam in 22 min, 32 min, 1 h 18 min, and 1 h 30 min, respectively, with an average travel speed of 0.5 to 2.5 km per minute. The rapid downstream water flow over short distances is demonstrated by the inverse relationship between discharge and distance from the dam.

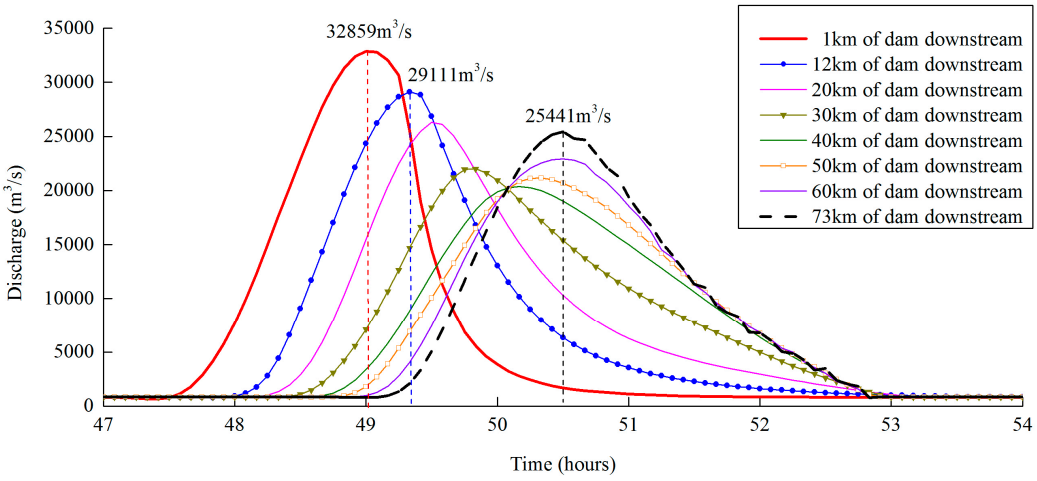

Figure 11. Flow discharge process of a one-way typical downstream section following the dam break.

3.5. Breach Parameter

Table 3 presents the travel duration of the flood and peak discharge at various downstream sections, assuming a breach time of 2 hours. The analysis was performed using the following parameters: the breach elevation was set at 410 m, with Karot Dam modeled as a dam-break structure. The dam had a crest length of 460 m and a crest elevation of 469.5 m.

Case I: A breach duration of 2 h and a breach width of 181 m

The peak discharge was 33,561 m^3/s at the dam break, with a breach time of 2 h and a width of 181 m. The peak flood at outlet was 28,187 m^3/s, occurring 4 h and 40 min after the simulation began.

Table 3. Travel duration of flood and peak discharge at different downstream sections with a breach time of 2 h.

Distance from Dam (km)	Travel Duration after the Simulation Begins (h)			Peak Discharge (m^3/s)		
	Breach width(m)			Breach width(m)		
0	181	256	331	181	256	331
	2 h	2 h	2 h	33,561	34,402	35,405
10	2 h 15 min	2 h 15 min	2 h 10 min	32,501	33,494	34,396
20	2 h 20 min	2 h 20 min	2 h 20 min	31,638	32,538	33,434
30	2 h 45 min	2 h 45 min	2 h 45 min	30,653	31,679	32,545
40	3 h 15 min	3 h 5 min	3 h 5 min	29,754	30,820	31,657
60	3 h 45 min	3 h 15 min	3 h 15 min	28,975	29,931	30,777
73	4 h 40 min	4 h 30 min	4 h 25 min	28,187	28,922	29,769

Case III: Breach duration of 2 h and a breach width of 331 m

The peak discharge was 35,405 m^3/s at the dam break, with a breach time of 2 h and a width of 331 m. The peak flood at outlet was 29,769 m^3/s after 4 h, and 25 min after the simulation began.

3.6. Model Calibration and Validation

The MIKE 11 HD model was set up to simulate river flow by establishing boundary conditions, incorporating the river's cross-sectional data, and defining initial discharge and water-level values. Model calibration was performed using data from the hydrodynamic (HD) module. Figure 12 illustrates a comparison between the calculated and measured discharge values. The discharge measurements were taken at the last cross-section of the river, downstream of Karot Dam. This location was chosen to evaluate the model's accuracy in predicting flow characteristics downstream. The results demonstrated that the model provided reliable discharge predictions, with a positive correlation between the measured water levels and the calculated discharge at the downstream location, evidenced by a correlation coefficient of $R^2 = 0.9653$.

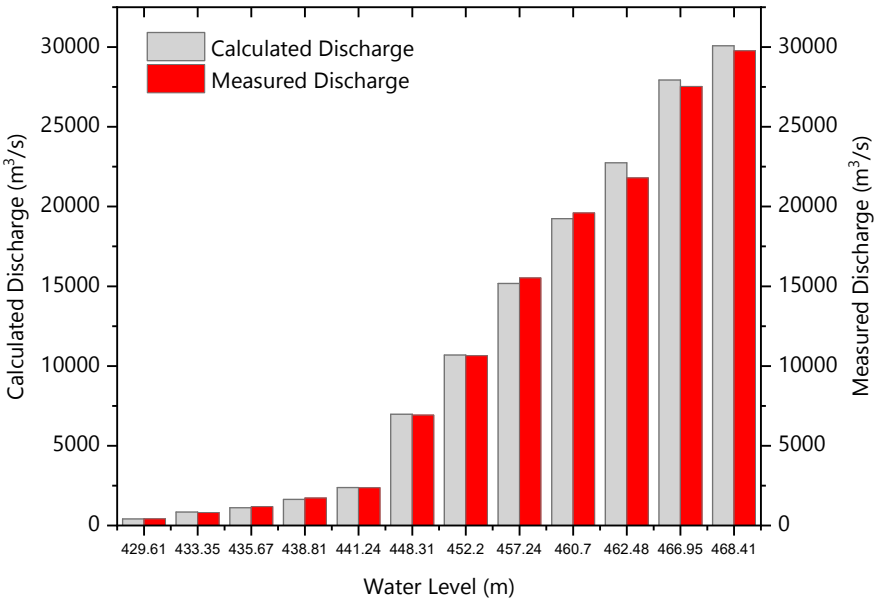

Figure 12. Comparison of measured and calculated discharge for the model at downstream of the dam.

4. Conclusions and Limitation of Study

4.1. Conclusion

This study demonstrates the use of the Danish Hydraulic Institute's (DHI) MIKE 11 hydraulic model, a one-dimensional unsteady flow model, to simulate flood behavior

downstream of the Karot Dam. The model considers various factors, such as breach parameters, flood duration, water depth, flow velocity, discharge rate, and downstream distance under average multi-year inflow conditions. The peak flow at the dam site was found to exceed the 10,000-year recurrence natural peak discharge of 32,300 m^3/s, with the dam failure producing a peak discharge of 33,171 m^3/s. Despite this significant increase, the breach lasted for only 2 h. Hydrodynamic model simulations were used to verify these findings, confirming the accuracy of the estimated peak flow and breach duration.

The results from empirical relationships and the MIKE 11 model were compared, and the following conclusions were drawn: For a breach time of 2 h, peak discharges were estimated at 33,561 m^3/s, 34,402 m^3/s, and 35,405 m^3/s for breach widths of 181 m, 256 m, and 331 m, respectively. Additionally, discharge flows reached the outlet in 4 h 40 min, 4 h 30 min, and 4 h 25 min for breach widths of 181 m, 256 m, and 331 m, respectively. The findings indicate that wider breaches lead to higher flood intensity downstream. Mangla Dam is safe from dam failure floods under multi-year average inflow conditions, with a maximum outflow of 12,097 m^3/s, which is lower than the normal spillway capacity of 30,147 m^3/s. The maximum water level is 378.56 m.

Flood control management and operational units should be equipped with necessary supplies and early warning systems. If a forecast suggests that Karot Dam may exceed its spillway capacity due to flooding, it is crucial to release water early to maintain the dam's safety. In the event of a dam collapse, the immediate evacuation of residents is imperative. Since floodwaters from a Karot Dam breach could quickly reach the downstream the Mangla Dam site, there may not be enough time for the Mangla Hydropower Station to release water before the flood's arrival. To address this challenge, it is recommended to enhance early warning forecasts and proactively release water when there is a potential risk of extremely high floods upstream at the Azad Pattan Hydrological Station.

4.2. Limitations of This Study

Regardless of the important conclusions highlighted above, the safety of dams can be significantly impacted by earthquakes, particularly in seismically active areas. Due to limited time and resources, this study does not cover earthquake impacts on rockfill dams. Thus, it is advised that, with the use of MIKE 11 or similar hydrodynamic modelling software, future research should take seismic analysis at Karot Dam into account. The findings will provide deeper insights into dam water dynamics and its interaction with the rock at the dam base, the expansion of construction joints, radiation damage in semi-unbounded rock, the compressibility of water in an impoundment, and variations in ground motions at different locations at the junction of the dam.

Author Contributions: Conceptualization, L.T.M. and C.L.; methodology, L.T.M.; software (Mike11:2014 version), F.N.M.M., L.T.M. and I.O.; validation, L.T.M., C.L., I.O. and M.R.; formal analysis, L.T.M.; investigation, F.N.M.M. and I.O.; resources, C.L.; data curation, M.R.; writing—original draft preparation, L.T.M.; writing—review and editing, L.T.M.; visualization, L.T.M.; supervision, C.L.; project administration, M.R. and I.O.; funding acquisition, L.T.M. All authors have read and agreed to the published version of the manuscript.

Funding: This research was funded by Open Research Program of Key Laboratory of Sediment Science and Northern River Training, the Ministry of Water Resources, China Institute of Water Resources and Hydropower Research under contract No. IWHR-SEDI-2023-07; Hubei Province Natural Science Foundation (General Program) under contract Nos 2023AFB594; Open Research Program of Hubei Key Laboratory of Construction and Management in Hydropower Engineering, China Three Gorges University under contract Nos 2024KSD20; National Natural Science Foundation of China under contract Nos 52009079; Major scientific and technological projects of the Ministry of Water Resources of China under contract Nos (SKS-2022003); Open Research Program of Key project of key laboratory in Hubei Province for water security in watershed under contract Nos (CX2023K13).

Data Availability Statement: The data presented in this study are available on request from the corresponding author.

Acknowledgments: Fund Project: Key Laboratory of Sediment Science and Northern River Training, the Ministry of Water Resources, China Institute of Water Resources and Hydropower Research (Grant Nos. IWHR-SEDI-2023-07); Hubei Province Natural Science Foundation (General Program) (2023AFB594); Hubei Key Laboratory of Construction and Management in Hydropower Engineering, China Three Gorges University (2024KSD20); National Natural Science Foundation of China Young Scholars Science(52009079); Major scientific and technological projects of the Ministry of Water Resources of China (SKS-2022003); Key project of laboratory in Hubei Province for water security in watershed (CX2023K13).

Conflicts of Interest: Frank N. M. Masami was employed by GITEC-IGIP in Association with ICE Project Services Limited, Simiyu Climate Resilience Project, Simiyu, Tanzania. The remaining authors declare that the research was conducted in absence of any commercial or financial relationships that could be construed as potential conflict of interest.

References

1. Azeez, O.; Elfeki, A.; Kamis, A.S.; Chaabani, A. Dam break analysis and flood disaster simulation in arid urban environment: The Um Al-Khair dam case study, Jeddah, Saudi Arabia. *Nat. Hazards* **2020**, *100*, 995–1011. [CrossRef]
2. Bharti, M.K.; Sharma, M.; Islam, N. Study on the Dam & Reservoir, and Analysis of Dam Failures: A Data Base Approach. *Int. Res. J. Eng. Technol.* **2020**.
3. Yi, X. A dam break analysis using HEC-RAS. *J. Water Resour. Prot.* **2011**, *3*, 370–379.
4. Cannata, M.; Marzocchi, R. Two-dimensional dam break flooding simulation: A GIS-embedded approach. *Nat. Hazards* **2012**, *61*, 1143–1159. [CrossRef]
5. Athens News. Available online: https://en.rua.gr/2023/02/06/cracks-in-the-ataturk-dam-after-earthquakes/ (accessed on 1 April 2023).
6. ACAPS. Impact of Storm Daniel in Eastern Libya and the Collapse of Dam in Derna. 2023. Available online: https://www.acaps.org/fileadmin/Data_Product/Main_media/20230913_ACAPS_thematic_report_Libya_impact_of_Storm_Daniel_in_eastern_Libya_and_the_collapse_of_dams_in_Derna.pdf (accessed on 10 September 2024).
7. Latrubesse, E.M.; Park, E.; Sieh, K.; Dang, T.; Lin, Y.N.; Yun, S.H. Dam failure and a catastrophic flood in the Mekong basin (Bolaven Plateau), southern Laos. *Geomorphology* **2020**, *362*, 107221. [CrossRef]
8. Rodrigues, A.S.; Santos, M.A.; Santos, A.; Rocha, F. Dam-break flood emergency management system. *Water Resour. Manag.* **2002**, *16*, 489–503. [CrossRef]
9. Feng, S.; Wang, W.; Hu, K.; Hoeg, K. Stress-strain-strength behavior of asphalt core in embankment dams during construction. *Constr. Build. Mater.* **2020**, *259*, 119706. [CrossRef]
10. Qiu, T.; Wang, W.; Höeg, K.; Feng, S.; Zhao, R. 3D analysis of the 174-m high Quxue asphalt-core rockfill dam in a narrow canyon. *Soils Found.* **2021**, *61*, 1645–1659. [CrossRef]
11. Tzenkov, A.D.; Kisliakov, D.S.; Schwager, M.V. An application of sophisticated FEM and simplified methods to the seismic response analysis of an asphalt-concrete core rockfill dam. In *Role of Dams and Reservoirs in a Successful Energy Transition*; CRC Press: Boca Raton, FL, USA, 2023. [CrossRef]
12. Jin, F.; Huang, D.; Lino, M.; Zhou, H. A Brief Review of Rock-Filled Concrete Dams and Prospects for Next-Generation Concrete Dam Construction Technology. *Engineering* **2024**, *32*, 99–105. [CrossRef]
13. Chen, C.; Zhang, L. Hydro-mechanical behavior of soil experiencing seepage erosion under cyclic hydraulic gradient. *Géotechnique* **2023**, *73*, 115–127. [CrossRef]
14. Xu, B.; Li, Y.; Pang, R. Plasticity inverse analysis for Zipingpu concrete-faced rockfill dam based on advanced cloud surrogate model via improved Jaya optimization algorithm. *Comput. Geotech.* **2023**, *160*, 105555. [CrossRef]
15. Li, C.W.; Li, A.Q.; Xu, Z.M.; Huang, Y. Sensitivity Analysis of Rock-fill Dam Break Flood on Different Dam Break Durations. *Open J. Saf. Sci. Technol.* **2021**, *11*, 89–103. [CrossRef]
16. Ministry of Water Resources, People's Republic of China. *2017 Statistic Bulletin on China Water Activities*; China Water & Power Press: Beijing, China, 2018.
17. Lu, J.; Guo, X.; Fu, H. Experimental investigation of breaching process of moraine dam with different breach-section shapes. *Environ. Earth Sci.* **2024**, *83*, 198. [CrossRef]
18. Feng, S.; Wang, W.; Hu, W.; Deng, Y.; Yang, J.; Wu, S.; Zhang, C.; Höeg, K. Design and performance of the Quxue asphalt-core rockfill dam. *Soils Found.* **2020**, *60*, 1036–1049. [CrossRef]
19. Li, Y.; Liu, H.; Wen, L. Reliability analysis of high core rockfill dam against seepage failure considering spatial variability of hydraulic parameters. *Acta Geotech.* **2024**, *19*, 4091–4106. [CrossRef]
20. Wong, T.L.X.; Hasan, M.R.M.; Peng, L.C. Recent development, utilization, treatment and performance of solid wastes additives in asphaltic concrete worldwide: A review. *J. Traffic Transp. Eng.* **2022**, *9*, 693–724. [CrossRef]
21. Ayati Ahmadi, A.; Noorzad, A.; MohammadNezhad, H.; Mirghasemi, A.A. Seismic Fragility of Rockfill Dams with Asphaltic Concrete Core. *Iran. J. Sci. Technol. Trans. Civ. Eng.* **2023**, *47*, 1585–1598. [CrossRef]

22. Roy, S.; Jain, V.K.; Gupta, M.; Chitra, R. Review of Use of Asphaltic Concrete Core in Earthen/Rock Fill Embankment Dam. In *Earth Retaining Structures and Stability Analysis*; Muthukkumaran, K., Umashankar, B., Pitchumani, N.K., Eds.; IGC 2021. Lecture Notes in Civil Engineering; Springer: Singapore, 2023; Volume 303. [CrossRef]
23. Alemie, N.A.; Wosenie, M.D.; Belew, A.Z. Performance evaluation of asphalt concrete core earth-rock fill dam relative to clay core earth-rock fill dam in the case of Megech Dam, Ethiopia. *Arab. J. Geosci.* **2021**, *14*, 2712. [CrossRef]
24. Sun, B.; Deng, M.; Zhang, S.; Wang, C.; Du, M. Seismic performance assessment of high asphalt concrete core rockfill dam considering shorter duration and longer duration. *Structures* **2022**, *39*, 1204–1217. [CrossRef]
25. Jacob, X.K.; Bisht, D.S.; Chatterjee, C.; Raghuwanshi, N.S. Hydrodynamic modeling for flood hazard assessment in a data scarce region: A case study of Bharathapuzha River basin. *Environ. Model. Assess.* **2020**, *25*, 97–114. [CrossRef]
26. Mei, S.; Zhong, Q.; Yang, M.; Chen, S.; Shan, Y.; Zhang, L. Overtopping-Induced breaching process of concrete-faced rockfill dam: A case study of Upper Taum Sauk dam. *Eng. Fail. Anal.* **2023**, *144*, 106982. [CrossRef]
27. Phyo, A.P.; Yabar, H.; Richards, D. Managing dam breach and flood inundation by HEC-RAS modeling and GIS mapping for disaster risk management. *Case Stud. Chem. Environ. Eng.* **2023**, *8*, 100487. [CrossRef]
28. Zhong, Q.; Wang, L.; Chen, S.; Chen, Z.; Shan, Y.; Zhang, Q.; Ren, Q.; Mei, S.; Jiang, J.; Hu, L.; et al. Breaches of embankment and landslide dams—State of the art review. *Earth-Sci. Rev.* **2021**, *216*, 103597. [CrossRef]
29. USACE. *Hydrologic Engineering Center's (HEC) Dam Failure Analysis*; U.S. Army Corps of Engineers: Washington, DC, USA, 2019.
30. Durmaz, S.; Ülgen, D. Prediction of earthquake-induced permanent deformations for concrete-faced rockfill dams. *Nat. Hazards* **2021**, *105*, 587–610. [CrossRef]
31. DHI. *MIKE 11—A Modelling System for Rivers and Channels, User's Manual*; Danish Hydraulic Institute: Horsholm, Denmark, 2022.
32. DHI. *MIKE 11: A Modelling System for Rivers and Channels, Reference Manual*; Danish Hydraulic Institute: Horsholm, Denmark, 2008.
33. Ministry of Water Resources. *Regulation for Calculating Design Flood of Water Resources and Hydropower Projects (SL44-2006)*; Ministry of Water Resources: Beijing, China, 2006.
34. *SL 164-2010*; Regulations for Simulation of Dam-Break Flow. Ministry of Water Resources: Beijing, China, 2010.